



# Drivers of Caribbean precipitation change due to global warming: analyses and emergent constraint of CMIP6 simulations

Marta Brotons<sup>1,5</sup> · Rein Haarsma<sup>1,2</sup> · Nadia Bloemendaal<sup>1,3</sup> · Hylke de Vries<sup>1</sup> · Teddy Allen<sup>4</sup>

Received: 26 May 2023 / Accepted: 17 December 2023  
© The Author(s) 2024

## Abstract

Using 31 CMIP6 models we have analyzed projected future Caribbean precipitation. The model mean projection results in a 0.5 mm/day (20%) drying under a SSP5-8.5 scenario for the end of this century over the Caribbean basin. The multi-model spread is large ranging from no drying to a 1 mm/day (40%) reduction in mean precipitation. Eastern and central Pacific warming, resembling an El Niño / positive phase of Pacific Decadal Oscillation (PDO), appears to be the main driver by shifting and weakening the Walker circulation and inducing subsidence over the Caribbean, especially during the wet season (May–November). This applies for the model mean as well as for the inter-model spread. During the dry season (December–April) the southward migration of the Intertropical Convergence Zone (ITCZ) and the advection of dry air from outside the Caribbean seem to be the dominant drivers of the projected drying. Another mechanism that contributes to the drying is the land-sea contrasts that induce divergence/convergence over the Caribbean. The incapability of CMIP6 models to simulate the current tropical Pacific warming and Walker circulation trends questions the reliability of precipitation projections in the Caribbean. Based on our understanding of the physical processes affecting Caribbean drying and on an emergent constraint analysis we state that the future drying in the Caribbean is likely to be weaker than the one projected by CMIP6 models.

**Keywords** Precipitation · Caribbean · Projections · Large-scale dynamics

## 1 Introduction

The Caribbean is vulnerable to hydro-meteorological hazards like storms, floods, droughts, and tropical cyclones. The region's vulnerability is a consequence of factors such as small island size, topography, densely populated areas, low altitude of urban areas, strong dependence on rainwater, and climate sensitive industries like tourism, agriculture, and fisheries (Lewsey et al. 2004; Taylor et al. 2012). Moreover, due to their limited financial resources to overcome past impacts and mitigate future risks, many islands in the Caribbean are considered Small Islands Developing States (SIDS) (Bloemendaal and Koks 2022). The occurrence of extreme climate events affecting the Caribbean is likely to be exacerbated by climate change (Karmalkar et al. 2013; Climate Studies Group Mona (Eds.) 2020; Van Meerbeeck 2020). Because of the linkage of those extremes to large-scale atmospheric circulation, understanding of how climate change affects the Caribbean atmospheric circulation, and its variability is crucial for a reliable assessment of the impact of climate change on hydro-meteorological hazards.

---

✉ Marta Brotons  
m.brotons@meteo.uv.es

Rein Haarsma  
rein.haarsma@knmi.nl

Nadia Bloemendaal  
nadia.bloemendaal@vu.nl

Hylke de Vries  
hylke.de.vries@knmi.nl

Teddy Allen  
tallen@cimh.edu.bb

<sup>1</sup> Royal Netherlands Meteorological Institute (KNMI), Utrecht, The Netherlands

<sup>2</sup> Climate Lighthouse Consultancy, Utrecht, The Netherlands

<sup>3</sup> Free University of Amsterdam (VU), Amsterdam, The Netherlands

<sup>4</sup> Caribbean Institute for Meteorology and Hydrology (CIMH), Oxnards, Barbados

<sup>5</sup> Present Address: University of Barcelona (UB), Barcelona, Spain

We define the Caribbean as the region situated between 8°N to 24°N and 60°W to 90°W. The Caribbean region presents a complex hydro-climate affected by different processes. Martinez et al. (2019) identify four main systems that determine the moisture availability in the region: the North Atlantic Subtropical High (NASH), the Caribbean Low-Level Jet (CLLJ), the Eastern Pacific and Atlantic Intertropical Convergence Zone (ITCZ), and the Atlantic Warm Pool (AWP).

The southern flank of the NASH is characterized by easterly winds, which produce moisture divergence (dry conditions) in the absence of unstable upper tropospheric westerlies across the Caribbean. In contrast, its western flank features southeasterly winds, which produce moisture convergence (wet conditions) in the Caribbean. As a result, the location of the NASH affects the moisture availability in the Caribbean. During boreal winter and summer, the NASH causes strong easterlies and moisture divergence reducing moisture availability. Spring and fall are characterized by weaker easterlies over the Caribbean driving wetter conditions in the region (Wang 2007; Martinez et al. 2019). The CLLJ is associated with moisture transport from the Caribbean Sea and the Gulf of Mexico to the United States. Strengthening of the CLLJ produces moisture divergence in the Caribbean and the Gulf of Mexico and moisture convergence (precipitation) in the United States (Wang 2007). The genesis of the CLLJ appears to be related to the intensification of easterly winds by NASH (Wang 2007; Cook and Vizy 2010) and its strength and orientation to the AWP (Wang and Lee 2007) and NASH (Cook and Vizy 2010).

The ITCZ, located between 4 and 12°N in the surroundings of the Caribbean, migrates meridionally following the solar cycle (Waliser and Gautier 1993; Philander et al. 1996; Zhang 2001; Gu et al. 2005). When the ITCZ is located over the Caribbean, moisture convergence is enhanced, resulting in wetter conditions. Similarly, drier conditions occur when the ITCZ is located north or south of the Caribbean (Martinez et al. 2019).

During late spring and early summer, the AWP is present in the Gulf of Mexico but absent in the Caribbean Sea, hereby driving a local low sea level pressure (SLP) in the Gulf of Mexico and a local high SLP in the Caribbean. The SLP dipole produces a meridional SLP gradient which enhances trade winds and strengthens the CLLJ. Once the AWP has expanded to the whole region during late summer until early autumn, the meridional SLP gradient is not present anymore. Then, high sea surface temperatures (SSTs) favor lower SLP, which weakens the NASH and trade winds, enhancing moisture convergence and leading to wetter conditions (Wang 2007; Wang et al. 2008). The AWP is absent during winter.

The combination of the different seasonality of the systems that affect Caribbean rainfall, described above, leads

to the bimodal pattern of precipitation, with the exception of the Lesser Antilles (Martinez et al. 2019), and to four precipitation seasons. These are Winter Dry Season (WDS), from December to April; Early Rainy Season (ERS), from May to June; Mid-Summer Drought (MSD), from July to August and Late Rainy Season (LRS), from September to November (Giannini et al. 2000; Anthony Chen and Taylor 2002; Taylor et al. 2002; Allen and Mapes 2017; Martinez et al. 2019; Climate Studies Group Mona (Eds.) 2020).

On an interannual time scale, different drivers affect Caribbean rainfall. Several studies consider the El Niño Southern Oscillation (ENSO) to be one of the most important ones (Giannini et al. 2000; Giannini et al. 2001a, b, c; Alexander et al. 2002; Rodriguez-Vera et al. 2019). El Niño, the warm episode of the ENSO cycle which manifests during boreal winter, produces an eastward migration of the Pacific Walker circulation. Consequently, a zonal seesaw in SLP develops, consisting of an anomalously low SLP in the eastern equatorial Pacific and an anomalously high SLP over the equatorial Atlantic. This pattern induces a lower tropospheric convergent flow over the eastern equatorial Pacific and a divergent one over the Caribbean basin. The divergent flow is associated with dry conditions. The zonal seesaw in SLP also has an indirect effect on SST: higher than average SLP in the equatorial Atlantic decreases the meridional SLP gradient over the North Atlantic and, consequently, weakens the NASH, which produces a weakening of trade winds and higher SSTs in the equatorial Atlantic. The indirect SST effect is lagged by a season, and thus, it takes place in the spring following an El Niño event. As explained above, high SSTs in the tropical Atlantic enhance precipitation (Giannini et al. 2000; Giannini et al. 2001a; Giannini et al. 2001c,b). ENSO also affects tropical cyclone (TC) activity in the tropical Atlantic. During an El Niño event, vertical wind shear (VWS) is enhanced over the Atlantic basin, resulting in TC formation suppression (Gray 1984; Goldenberg and Shapiro 1996; Tartaglione et al. 2003; Klotzbach 2011b,a). During La Niña events, the atmospheric response is opposite, resulting in wet conditions in the Caribbean and more favorable TC formation conditions in the tropical Atlantic.

Another driver of interannual Caribbean rainfall variability is the North Atlantic Oscillation (NAO). This index represents the meridional pressure gradient between the NASH and the Icelandic low (Visbeck et al. 2001). A positive phase indicates stronger than normal NASH, hence stronger trade winds and thus dry conditions in the Caribbean. A negative phase consists of the opposite situation (Giannini et al. 2000).

Several studies (Giannini et al. 2000; Anthony Chen and Taylor 2002; Wang 2007; Martinez et al. 2020) analyze the combined effect of ENSO and NAO, which can have a stronger effect if the two signals interfere constructively. Studies also attribute inter-annual variability in the

Caribbean to other drivers such as the Atlantic Multidecadal Oscillation (AMO) (Mendez and Magaña 2010; Klotzbach 2011b), the Pacific Decadal Oscillation (PDO) (Mendez and Magaña 2010; Chang and Oey 2013) and temperature gradients (Taylor et al. 2011; Chang and Oey 2013; Rodriguez-Vera et al. 2019). The Madden-Julian Oscillation (MJO) has been assigned as a mode dominating intra-seasonal variability of the region (Martin and Schumacher 2011). However, researchers have strong agreement considering ENSO and NAO as the dominant mechanisms affecting interannual variability in the Caribbean region.

Besides all efforts studying the drivers of precipitation in the Caribbean under current climate conditions, there is a lack of understanding of large-scale atmospheric dynamics affecting precipitation under future climate conditions. Coupled Model Intercomparison Project Phase 6 (CMIP6) models (Eyring et al. 2016) project an increase in drought severity and prevalence across the Caribbean region. (Cook et al. 2020; Almazroui et al. 2021; Herrera et al. 2020). For the end of the twenty-first century, CMIP6 models project a strong reduction in precipitation in the Caribbean region (around  $-0.5$  mm/day which equals approximately  $-20\%$ ). However, there is a large inter-model spread, projections range from nearly no reduction to a reduction up to 1 mm/day which is approximately 40% (Fig. 1).

This study aims to contribute to the understanding of precipitation projections in the Caribbean by analyzing an ensemble of 31 CMIP6 models, identifying the main processes responsible for the model mean trends and the inter-model spread. For this, we investigate the changes in atmospheric circulation and Caribbean moisture convergence that

induce the model mean drying and the inter-model spread, and the drivers of these changes. These changes and drivers will be linked to those governing the seasonal and interannual variability of Caribbean rainfall. In addition, we will analyze the reliability of the projected precipitation trends based on the comparison of the trends of the drivers of CMIP6 historical simulations with observations. Based on this analysis we will apply an emergent constraint analysis narrowing the projected drying. Although drought has many aspects, including hydrological drought, we focus here only on the dynamics affecting the precipitation.

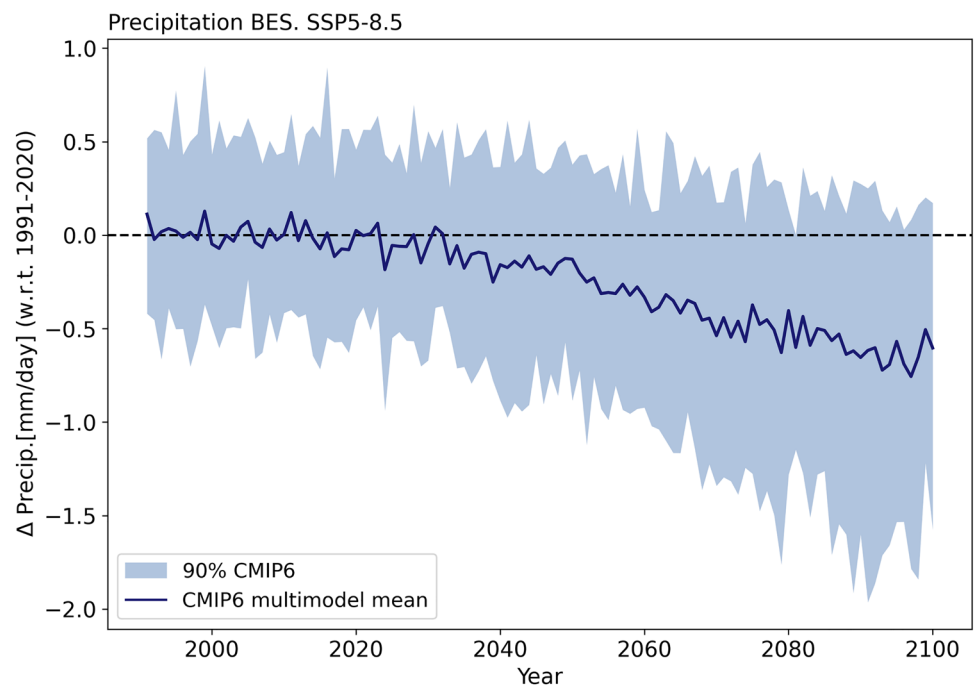
## 2 Data and methods

### 2.1 Data

For precipitation observations we use the MSWEP v2.8 (Beck et al. 2019), ERA5 reanalysis (Herrera et al. 2020) and Global Precipitation Climatology Project (GPCP) (Angeline 2016) Gridded Precipitation Products (GPPs). Centella-Artola et al. (2020) extensively analyzed different GPPs and found that MSWEP is one of the most reliable ones for the Caribbean region. This motivates us to base the spatial model validation for precipitation only on MSWEP.

For SSTs observations we use three different gridded datasets: the HadISST from the Met Office Hadley Centre (Rayner et al. 2003), ERA5 reanalysis data from the Copernicus Climate Change service Climate Data Store (Herrera et al. 2020) and the International Comprehensive Ocean-Atmosphere Data Set (ICOADS) (Freeman et al.

**Fig. 1** CMIP6 change in (yearly mean) precipitation projections averaged over the Caribbean region ( $8^{\circ}\text{N}$ – $24^{\circ}\text{N}$  and  $60^{\circ}\text{W}$ – $90^{\circ}\text{W}$ ). The output from 31 CMIP6 models (Table B.1) from historical and SSP5-8.5 simulations is used. The change is computed relative to the 1991 to 2020 average. The thick blue line represents the multi-model mean, while the shaded light blue region shows the 90% inter-model spread



2017) from National Oceanic and Atmospheric Administration (NOAA). ERA5 is also used to validate the models' vertical and horizontal velocities.

We use CMIP6 (Eyring et al. 2016) to analyze the impact of climate change. For the historical (from 1850 to 2014) simulations, we analyze the period from 1961 until 2014. Regarding the Shared Socioeconomic Pathways (SSPs or scenarios), only CMIP6 SSP5-8.5 emissions scenario simulations are taken due to a larger signal to noise ratio which facilitates the recognition and interpretation of the changes in the atmospheric dynamics. This choice is based on the pattern scaling hypothesis (Santer et al. 1990) which assumes that the dominant response will change in amplitude but not in pattern depending on the forcing scenario. In total, we use 31 CMIP6 models. The list of the models used together with their variant labels and their nominal resolutions are displayed in Table B.1. Monthly averages are used. The Climate and Forecast (CF) standard names, abbreviations, and units of the variables used are listed in Table B.2.

## 2.2 Methods

Our purpose is to obtain a comprehensive understanding of the main drivers dominating the Caribbean climate change in the multi-model mean and the inter-model spread of CMIP6 models. It is essential to note that our focus is not on the detailed examination of individual climate models. Consequently, this approach leads to several key simplifications. Firstly, we use monthly averaged data rather than data with higher temporal resolution. Secondly, our analysis encompasses the Caribbean region as a whole, although we realize its heterogeneity in precipitation patterns, as shown by Martinez et al. (2019). The latter simplification is also supported by the rather homogeneous climate change signal of the models over the Caribbean, as will be shown in Sect. 3. Furthermore, the large-scale and slowly evolving nature of the drivers affecting Caribbean climate provide additional bolstering to these simplifications.

To compare CMIP6 models' output we regrid all the models to a  $1^\circ \times 1^\circ$  spatial resolution using bilinear interpolation methods. We first conducted a model validation analysis for the current climate, focusing on precipitation. Validation is made for the reference period (1991 to 2020) for which we use a blend of historical (1991–2014) and SSP5-8.5 (2015–2020) simulations for the models. We compute precipitation climatologies from CMIP6 models and MSWEP. In addition, we compute the CMIP6 precipitation bias, defined as precipitation from CMIP6 models minus precipitation from MSWEP for the same period. We use a two-tailed Student t-test to study the significance of the CMIP6 multi-model mean bias. It could be argued that a land- only and an ocean-only model validation is necessary due to the different processes affecting Caribbean precipitation as a

consequence of topography. However, land vs. ocean validation is non-sense due to a double reason. First, most of the islands can not be resolved in CMIP6 models due to the coarse spatial resolution. Second, the drivers of Caribbean climate are mostly large-scale. A detailed spatial analysis of the precipitation bias for the islands is therefore out of the scope of this study and not possible.

To analyze the response of the climate system to different warming levels we need to eliminate the climate sensitivity of CMIP6 models. Thus, we set all the models to the same warming level by dividing the future change of the different variables by the increase in temperature averaged over the area between  $40^\circ\text{S}$  and  $40^\circ\text{N}$ . The new variables are referred to as the scaled variables. The motivation to choose the temperature in this latitude range instead of the change in global temperature comes from the assumption that the polar regions have little effect on the circulation in the tropics, whereas the temperature increase there is large. However, results are not sensitive to this choice since the output figures do not show major differences depending on the temperature used to scale the variables.

To analyze the change in atmospheric dynamics for a range of variables, we compute the difference between the mean of the reference period (1991–2020) and the mean of the future period (2071–2100). We then use a two-tailed Student t-test to examine the statistical significance of the multi-model change.

## 2.3 Moisture budget analysis

Following Martinez et al. (2019) we perform a moisture budget analysis for the Caribbean. The atmospheric moisture budget equation is:

$$P - E = -\frac{1}{g} \nabla \cdot \int_0^{p_s} q \mathbf{V} dp \quad (1)$$

where  $P$  is precipitation ( $\text{kg}/\text{m}^2\text{s}$ );  $E$  is evaporation ( $\text{kg}/\text{m}^2\text{s}$ );  $g$  is gravity ( $9.8 \text{ m}/\text{s}^2$ );  $q$  is specific humidity ( $\text{kg}/\text{kg}$ );  $\mathbf{V}$  is the wind field ( $\text{m}/\text{s}$ ), and  $p$  is pressure ( $\text{hPa}$ ). Because we focus on seasonal time scales, the storage capacity of the atmosphere is neglected. Taking the time mean of Eq. 1 and separating the total moisture flux convergence into a mean and transient term results in Eq. 2, where the mean flow convergence is the first term of the right-hand side (r.h.s.) and the transient convergence is the second term of the r.h.s.:

$$\overline{P} - \overline{E} \approx -\nabla \cdot \int_0^{p_s} \overline{\mathbf{V}q} \frac{dp}{g} - \nabla \cdot \int_0^{p_s} \overline{\mathbf{V}'q'} \frac{dp}{g} \quad (2)$$

where an overbar denotes time mean and primes denote daily departures from the time mean. Since we use monthly data, it is not possible to compute the convergence by the transient flow (second term on the r.h.s. of Eq. 2). However, Martinez



et al. (2019) find in their study that the contribution by this term over the Caribbean is minor south of 20°N. Since our study region is located south of this latitude, we decide to neglect the convergence by the transient flow. This reduces Eq. 2 to:

$$\bar{P} - \bar{E} \approx -\nabla \cdot \int_0^{p_s} \bar{\mathbf{V}} \bar{q} \frac{dp}{g} \tag{3}$$

Decomposing the r.h.s. of Eq. 3 gives:

$$-\nabla \cdot \int_0^{p_s} \bar{\mathbf{V}} \bar{q} \frac{dp}{g} = -\int_0^{p_s} (\bar{q} \nabla \cdot \bar{\mathbf{V}}) \frac{dp}{g} - \int_0^{p_s} (\bar{\mathbf{V}} \cdot \nabla \bar{q}) \frac{dp}{g} \tag{4}$$

where we will denote the first term of the r.h.s. the mass convergence and the second term of the r.h.s. the advection term.

Because of the minor contribution of the upper troposphere to moisture budget, the computation has been limited to lower pressure layers. Specifically, the three pressure layers (1000–925 hPa, 925–850 hPa and 850–700 hPa) have been used to approximate the integrals. This approximation for the computation of the moisture budget has been tested for one single model by comparing the results with those including all model layers, resulting in small differences (not shown). Results are obtained in kg/m2s, and subsequently converted to mm/day.

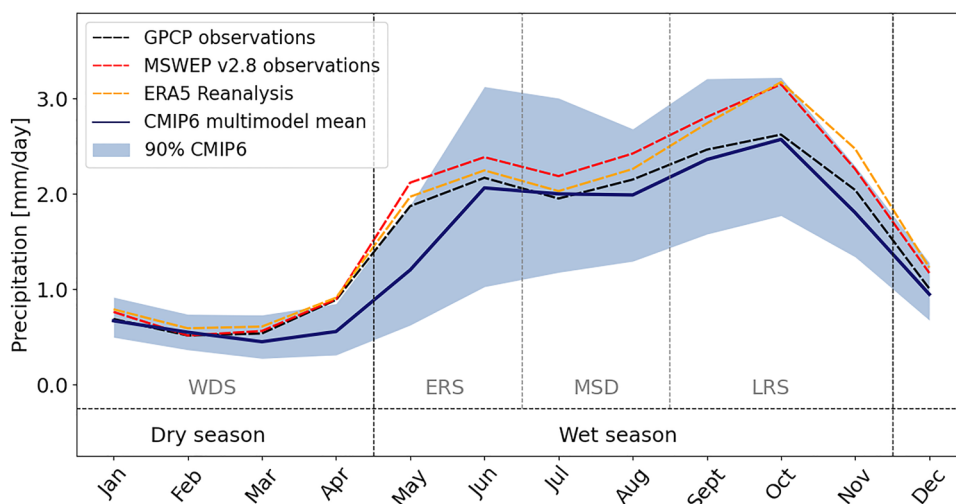
### 3 Model validation

Figure 2 shows the monthly averages of precipitation for the reference period from MSWEP, ERA5 and GPCP observations (dashed red, orange and black lines, respectively), the multi-model mean of CMIP6 (blue line) and the 90% spread of CMIP6 models (light blue shaded region). The

values shown correspond to spatial averages of the Caribbean region. From Fig. 2, we observe that CMIP6 models' mean slightly underestimates precipitation compared to the observations' ensemble. The precipitation underestimation is greater during the ERS. Moreover, we realize CMIP6 show a large spread in the climatology suggesting that models might be characterized by different climate regimes. As already mentioned, analyzing the individual models' climates is not the goal of our work, but understanding the dynamics governing CMIP6 models' future climates is. As such, from here on, we group the seasons into a dry and wet season, with the dry season being composed of the WDS, and the wet season being composed of the ERS, MSD and LRS. The division into two seasons still characterizes the major aspects of the climatology in the Caribbean and can be reliably simulated by CMIP6 models. In addition, the large-scale nature of the dynamics governing Caribbean climate provides another argument to consider the use of two seasons to be sufficient time resolution.

Figure 3 shows the model mean CMIP6 precipitation bias for the reference period. We observe an underestimation of precipitation over the western equatorial Pacific, and an overestimation in the western subtropical Pacific. Furthermore, in the eastern equatorial Pacific and Atlantic, models overestimate precipitation, indicating that in CMIP6 models, the ITCZ migrates excessively southward in those regions. Over land areas of the Caribbean models underestimate precipitation by a maximum of -5.73 mm/day (-55.7%) compared to MSWEP. The patterns observed in Fig. 3 resemble the double ITCZ bias and aligns with the findings of Adam et al. (2020), Tian and Dong (2020), and Si et al. (2021). The double ITCZ bias consists of an overestimation of precipitation over the southeastern Pacific and has been a long-standing bias in climate models (Zhang 2001; Zhang et al. 2015; Adam et al. 2020).

**Fig. 2** Rainfall climatologies averaged per month of the year and over the Caribbean region (8°N–24°N and 60°W–90°W). The period used is from 1991 to 2020. The black line shows data from GPCP observations, the blue line shows the multi-model mean of the 31 CMIP6 models and the shaded area is the 90% spread. Gray vertical dashed lines delimit the four seasons: Winter Dry Season (WDS), Early Rainy Season (ERS), Mid-Summer Drought (MSD), and Late Rainy Season (LRS) and black vertical dashed lines limit the wet and dry seasons encompassing the four seasons



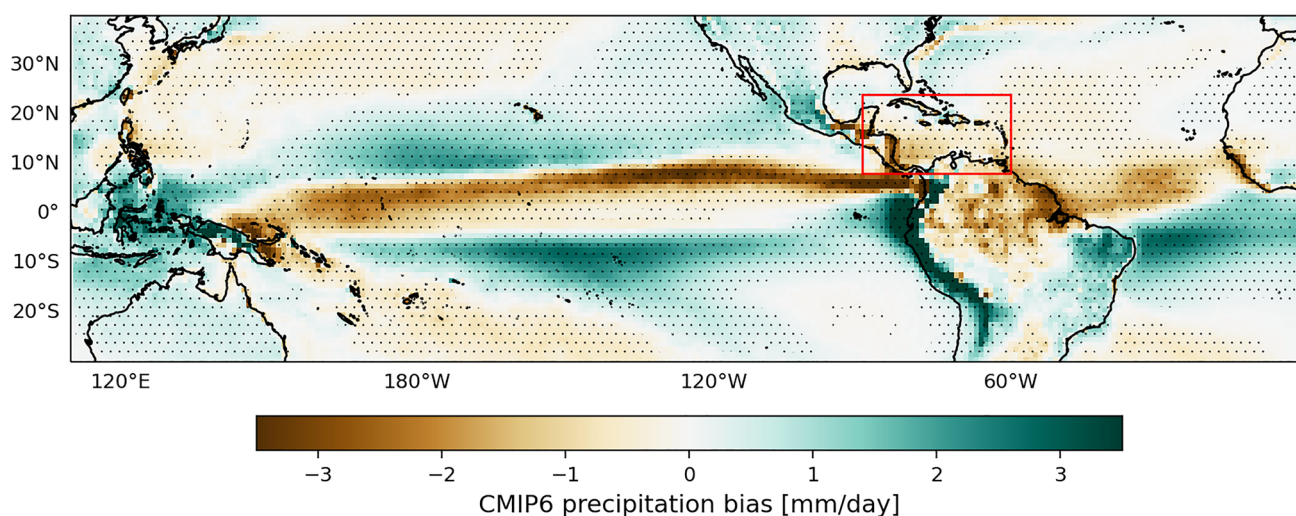


**Fig. 3** Annual mean of the CMIP6 precipitation bias (using MSWEP v2.8 as observations). Results are shown for the 1991 to 2020 period. Hashing shows the regions where the multi-model mean bias is significant at the 95% confidence level. The Caribbean region is marked

with a red box. Positive values indicate an overestimation of precipitation by CMIP6 models while negative values show an underestimation

Although many of those biases, such as the double ITCZ, are common to all CMIP6 models there is also a large spread between the models as can be seen in Fig. 2 and Fig. 14. From the latter figure it is notable that especially over the Caribbean region the spread in the bias among the models is large.

## 4 Projections

### 4.1 Model mean Caribbean drying

#### 4.1.1 Circulation changes

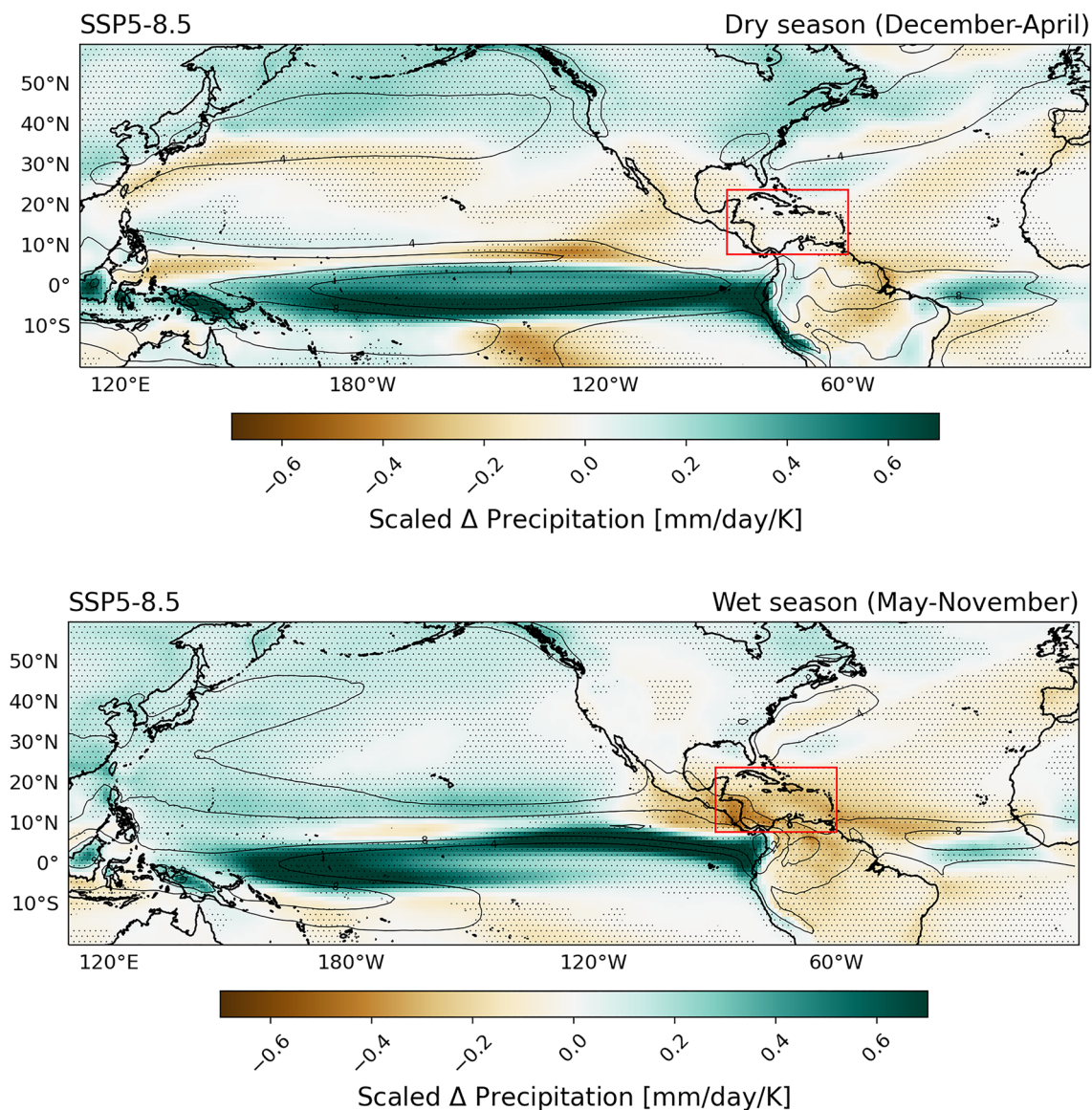
To investigate the change in atmospheric circulation at the end of the century and the drivers of the Caribbean drying trend, we compute the multi-model mean scaled change for different variables (see Sect. 2.2).

Figure 4 shows the scaled change in precipitation for the dry and the wet season on the upper and the lower panels, respectively. We see that both seasons are characterized by an increase of precipitation in the equatorial tropics and a decrease in the subtropics, specially in the North Atlantic. These patterns are similar to the ones from the Summary for Policymakers of the IPCC AR6 (Masson-Delmotte et al. 2021). Over the Caribbean region, CMIP6 models show a homogeneous drying for both seasons with a larger amplitude during the wet season. For the dry season (Fig. 4a), the strongest drying is located west of the Caribbean around 150°W to 120°W and 10°N.

In Fig. 4b we observe a drying in the North Atlantic Convergence Zone (NACZ) while, a wetting is observed in the North Pacific Convergence Zone (NPCZ). Thus, suggesting a future climate characterized by zonal flow from the tropical Atlantic toward the tropical Pacific which advects moisture from the NACZ to the NPCZ. In Fig. 4 we also identify a drying around 10°N latitude and a wetting around 0°N which are larger during the dry season. This dipole in the sign of precipitation indicates a southward migration of the ITCZ. To further investigate these hypotheses and understand their drivers we must look at different variables.

Similar to the biases, the CMIP6 precipitation projections show a large spread among the different models (Fig. 15), in particular over the Caribbean. The causes of this large spread, also reflected in Fig. 1, will be discussed below in Sect. 3.2.2.

To investigate the changes in atmospheric circulation that are responsible for the model mean change in precipitation at the end of the century, we analyze the changes in vertical velocity and wind. The change in scaled model mean omega at 500 hPa (colors) and wind at 850 hPa (vectors) are shown in Fig. 5. An increase in the upward motion over the NPCZ, for both seasons, and a decrease over the NACZ, during the wet season, are observed. This reflects an increase (decrease) in deep convection over the NPCZ (NACZ), which produces the observed increase (decrease) in precipitation in Fig. 4. During the wet season, an increase in downward motion occurs in the Caribbean. This subsidence over the Caribbean, accompanied by horizontal divergence and increased trade winds, reduces precipitation. The increase of downward motion over the Caribbean jointly with the increase



**Fig. 4** Scaled change in precipitation (in mm/day/K) at the end of the century (from 2071 to 2100) with respect to the reference period (from 1991 to 2020). Positive values indicate a future increase in precipitation and negative values correspond to a future decrease in precipitation. The contour lines show the reference period’s mean precipitation.

The dry and the wet seasons are shown in the upper and lower panel, respectively. Results shown are from the multi-model mean of the 31 CMIP6 models. Hashing shows the areas where the multi-model mean future change is significant at the confidence level over 95%. The red box shows the Caribbean region

of upward motion over the central Pacific, during the wet season, indicates an eastward migration of the Walker circulation that is associated with the drying trend in the Caribbean. This will be discussed extensively in the *Drivers of Caribbean drying Section*.

During the dry season the vertical motion over the Caribbean reveals an upward increase, while west of the Caribbean, there is a downward increase. Thus, suggesting that changes in the Walker circulation and its associated vertical motion are not responsible for a drier Caribbean. In addition, changes in the horizontal circulation are minor and much

less compared with the wet season. The future drying over the Caribbean during the dry season is therefore not due to changes in atmospheric circulation. The mechanism driving the dry season drying will be discussed in more detail in the next Section.

#### 4.1.2 Moisture budget changes

To further investigate the relative contribution of circulation driven and advection driven changes of the drying over the Caribbean we follow the approach of Martinez et al. (2019),



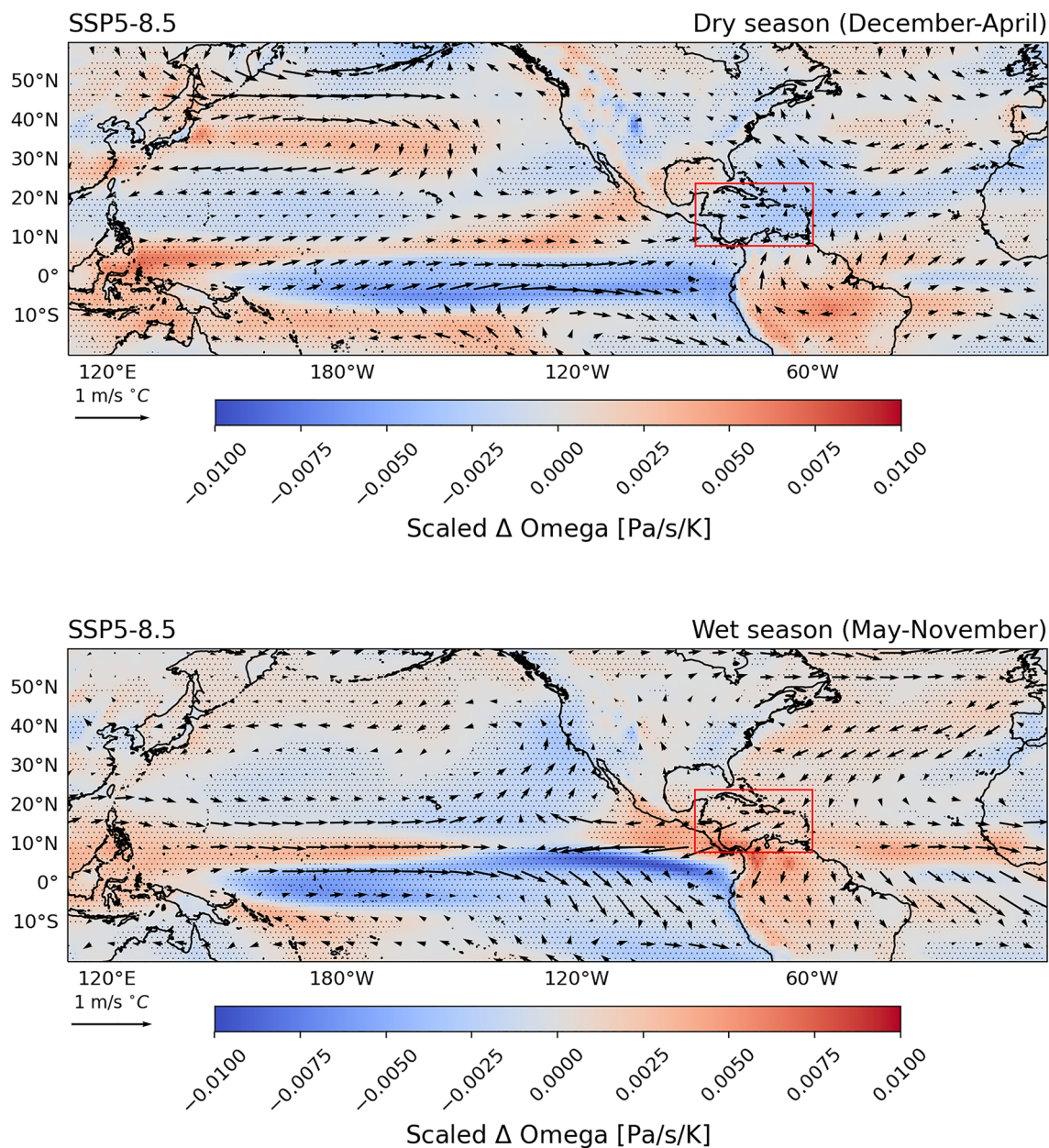


**Fig. 5** Same as Fig. 4 but for omega at 500 hPa (in colors, and in Pa/sK) and in wind at 850 hPa (in vectors, and in m/s/K)

by analyzing the moisture budget equation (see Sect. 2.3). As shown by Martinez et al. (2019) and discussed in Sect. 2.3 the moisture convergence over the Caribbean is dominated by the mean flow. We therefore neglect changes in the contribution from the eddy terms.

Figure 6 shows the changes in the moisture convergence (term on the l.h.s. of Eq. 4) (Fig. 6a, b) and the contributions from the change in the mass convergence (first term on the r.h.s. of Eq. 4) (Fig. 6c, d) and the moisture advection (second term of the r.h.s. of Eq. 4) (Fig. 6e, f). We checked the correctness of the computations of the moisture convergence by comparing them with the changes in P-E (Fig. 16).

During the wet season there is a clear reduction of moisture convergence over the Caribbean (Fig. 6b), which is dominated by changes in mass convergence (Fig. 6d), underscoring the importance of changes in atmospheric circulation discussed before. During the dry season the reduction in moisture convergence is less (Fig. 6a) and is dominated by the change in mass convergence as well (Fig. 6c). Although moisture advection during the dry season (Fig. 6e) seems to have a larger contribution on the moisture convergence. We observe a dipole in the mass converge which resembles a similar one identified in precipitation (Fig. 4). This indicates that the southward displacement of the ITCZ might

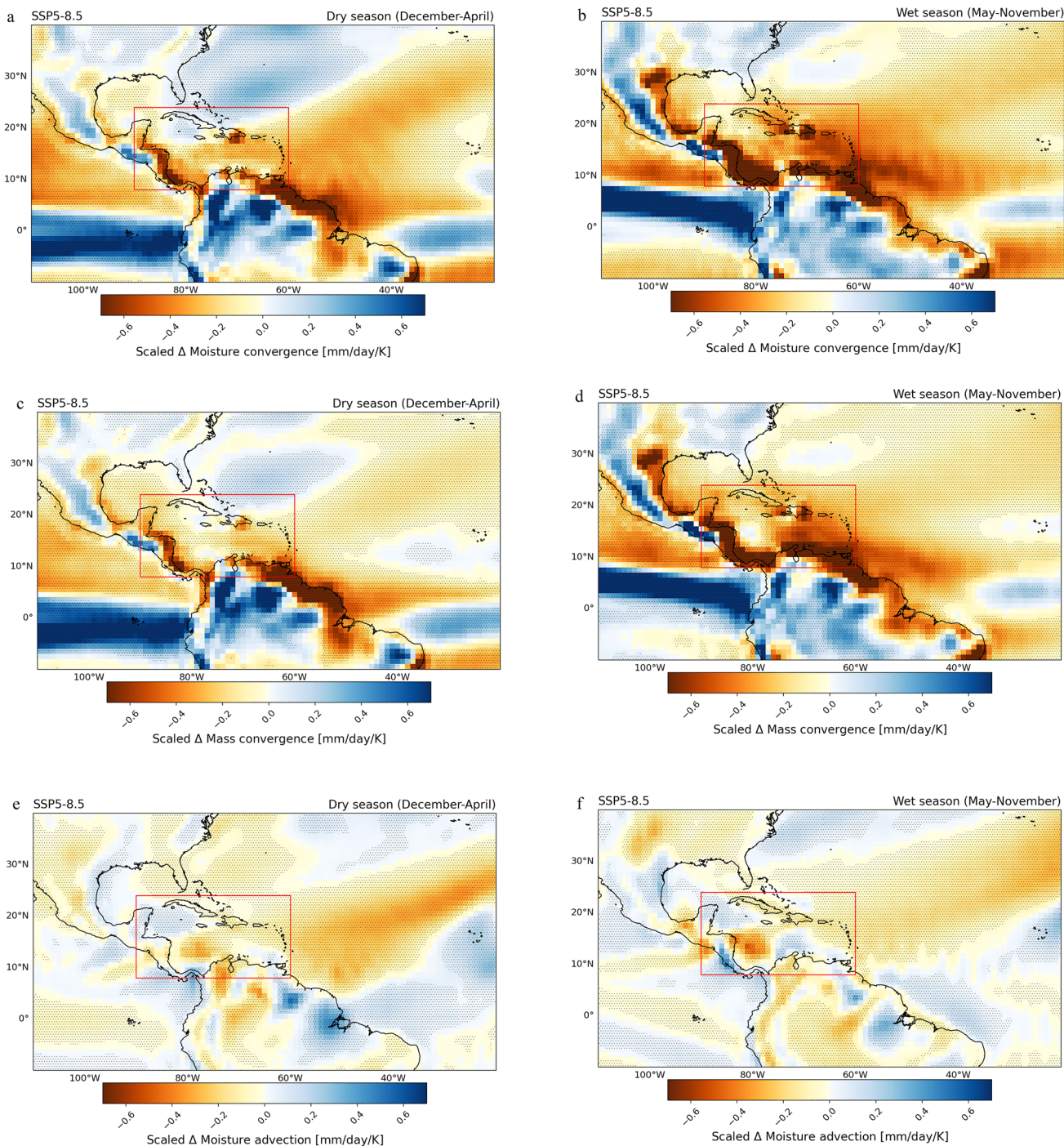


**Fig. 6** Same as Fig. 4 but for moisture convergence (a,b), mass convergence (c,d) and moisture advection (e,f) in *mm/day/K*

contribute to the mass convergence reduction. The drivers of the migration of the ITCZ will be discussed later. The advection term might be dominated by the trade winds and the CLLJ that advect the dry air from the neighboring areas to the Caribbean). A detailed analysis of the causes for the drying outside the Caribbean is outside the scope of this paper but enhanced downward motion in areas neighboring

the Caribbean such as the tropical Atlantic and west of the Caribbean (Fig. 5) contribute to this.

### 4.1.3 Drivers of Caribbean drying

To understand what drives the observed changes in precipitation and atmospheric circulation, we analyze near surface



temperature projections. Figure 7 shows the change in scaled temperature at 2 m for the dry season (upper panel) and the wet season (lower panel). Different regions of enhanced and reduced warming can be identified in Fig. 7. Most notably is the stronger warming over the Arctic region that is known as polar amplification and it is a consequence of the ice-albedo feedback and other effects (Holland and Bitz 2003; Pithan and Mauritsen 2014). The stronger warming over

land compared to ocean has been ascribed to the different lapse rates between ocean and land as the dominant cause (Joshi et al. 2008; Brogli et al. 2021).

The enhanced warming in the eastern tropical Pacific is most relevant for the observed changes in omega and the trade winds in the tropical Pacific and the Caribbean. The enhanced warming over the eastern tropical Pacific resembles the pattern of the warm phase of ENSO, also known

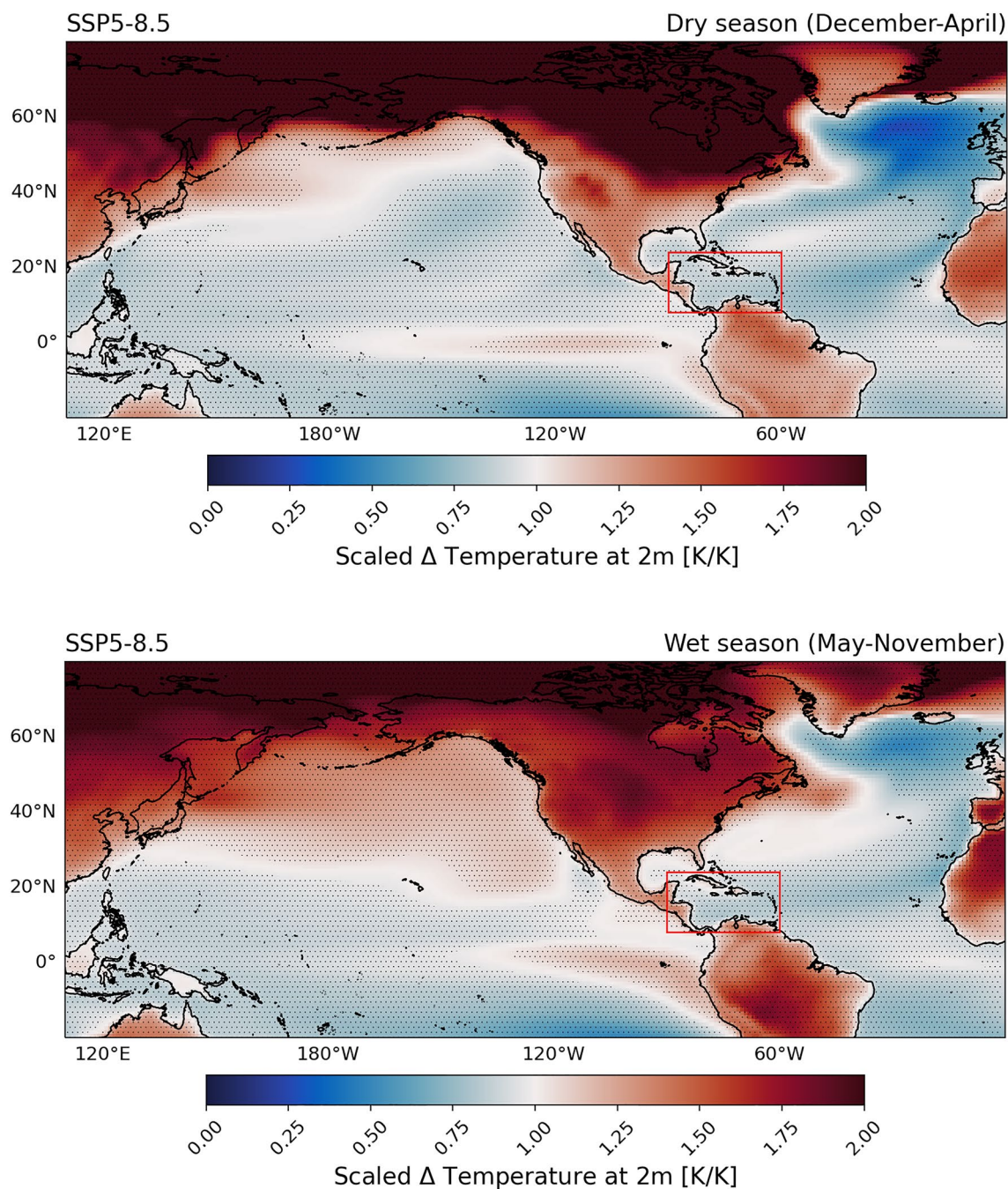


**Fig. 7** Same as Fig. 4 but for temperature at 2 m. Values higher than one indicate warming faster than the 40°N and 40°S region, while values below one show a weaker warming than that region

as El Niño. It should be noted that this does not indicate an increase in El Niño events, because we are analyzing 30-year averages. It, however, indicates a change in the tropical atmospheric circulation towards El Niño-like dynamics under global warming. The stronger warming in the central-eastern tropical Pacific produces the observed eastward migration of the convergence zone of the west Pacific and thus drives the eastward migration and weakening of the Walker circulation (Giannini et al. 2000, 2001c; Alexander et al. 2002; Rodriguez-Vera et al. 2019). Consequently, the downward branch of the Walker circulation is located over the Caribbean during the wet season (Fig. 5) driving the decrease in precipitation (Fig. 4). During the dry season, the downward branch is located west of the Caribbean (Fig. 5) and therefore the eastward migration of the Walker circulation does not drive the precipitation decrease in the dry season as already discussed before. The eastward migration of the Walker circulation also justifies the wetting of the NPCZ and drying of the NACZ due to changes in low level zonal winds.

Other drivers that may impact the Caribbean precipitation are the horizontal temperature gradients. In Fig. 7a strengthening of the gradient between the relative cool Caribbean Sea and relative warm South American continent can be observed, especially during the wet season. This gradient drives a divergent flow in the Caribbean and a convergent flow in South America which can be observed in the wind vectors in Fig. 5. Divergent flow over the Caribbean is associated with dry conditions (Taylor et al. 2011). Easterly winds driving the divergent flow of the Caribbean might also be enhanced by the zonal temperature gradient between the tropical Pacific and Atlantic during the wet season.

In addition, an increase in the eastern subtropical Pacific—southwestern North America temperature gradient is identified during the dry season. This temperature gradient is related to the North American monsoon dynamics. An increase in the gradient enhances southwesterly winds in Mexico and southwestern North America (Fig. 5a) and produces moisture convergence and precipitation in both regions (Adams and Comrie 1997). This might contribute to the weaker drying during the dry season (Fig. 4a).

Figure 7 also reveals a dipole over the tropical Atlantic with a less warming north of the equator that extends into the Caribbean and a more warming south of the equator. This dipole and in particular the subtropical Atlantic warming south of the equator displaces the ITCZ southward (Bellomo et al. 2021) as reflected by the dipole sign of precipitation changes over the tropical Atlantic (Fig. 4). The moisture budget analysis indicates that the southward migration of the ITCZ reduces mass convergence into the Caribbean region and is the main cause of drying during the dry season (Fig. 6). In addition Fig. 7 reveals less warming over the North Atlantic subpolar gyre. This warming hole has

been associated with a weakening of the Atlantic Meridional Overturning Circulation (AMOC) (Drijfhout et al. 2012) and a reduction of poleward heat transport (Rahmstorf et al. 2015; Caesar et al. 2018) that cools the North Atlantic and warms the South Atlantic. Our hypothesis is that the meridional temperature dipole over the tropical North Atlantic in Fig. 7 is induced by a weakening of the AMOC, although further analyses of the AMOC are needed to confirm this hypothesis. The dipole drives the meridional temperature gradient at the equator that produces the southward displacement of the ITCZ thus affecting precipitation.

## 4.2 Caribbean inter-model spread

To study the inter-model spread, we separate the CMIP6 models into dry and wet models. We define wet and dry models as models that are wetter than the 70th percentile and dryer than the 30th percentile, respectively, based on annual mean precipitation. In Table B.1 the models belonging to the wet and dry groups are indicated with green and brown text, respectively. The nominal atmospheric and oceanic resolutions are also listed in the table which permits us to conclude that there is not a clear linkage between the amplitude of the drying and the models' resolution. Figure 8 shows the scaled change in precipitation averaged over the Caribbean region for every model, together with the 30th and 70th percentile of the distribution. We see that most of the models project a drying in the Caribbean region under global warming, but that there is a large inter-model spread ranging from weak to strong drying, confirming the analyses of Fig. 1.

After defining the wet and dry models, the multi-model mean of the scaled changes of different variables for both groups and their difference (dry–wet) are calculated. This procedure is similar to the one used in Bellomo et al. (2021) but we use annual change of precipitation to divide the models in two groups.

### 4.2.1 Circulation differences

Figure 9 shows the difference between dry and wet models for the scaled change in precipitation. We see that the difference in precipitation between dry and wet models is largest in the Caribbean region. This is to be expected since the dry and wet group definition is based on precipitation change over the Caribbean. The patterns of Fig. 9 over the tropics are similar to those from Fig. 4 suggesting that the mechanisms driving the multi-model drying might also be responsible for the inter-models spread. During the wet season, there is a strong enhanced drying over the Caribbean that extends over the subtropical Atlantic for the dry models. This is less visible for the dry season. During the wet season there is enhanced precipitation over the NPCZ that is strongest in the western part. An additional band of

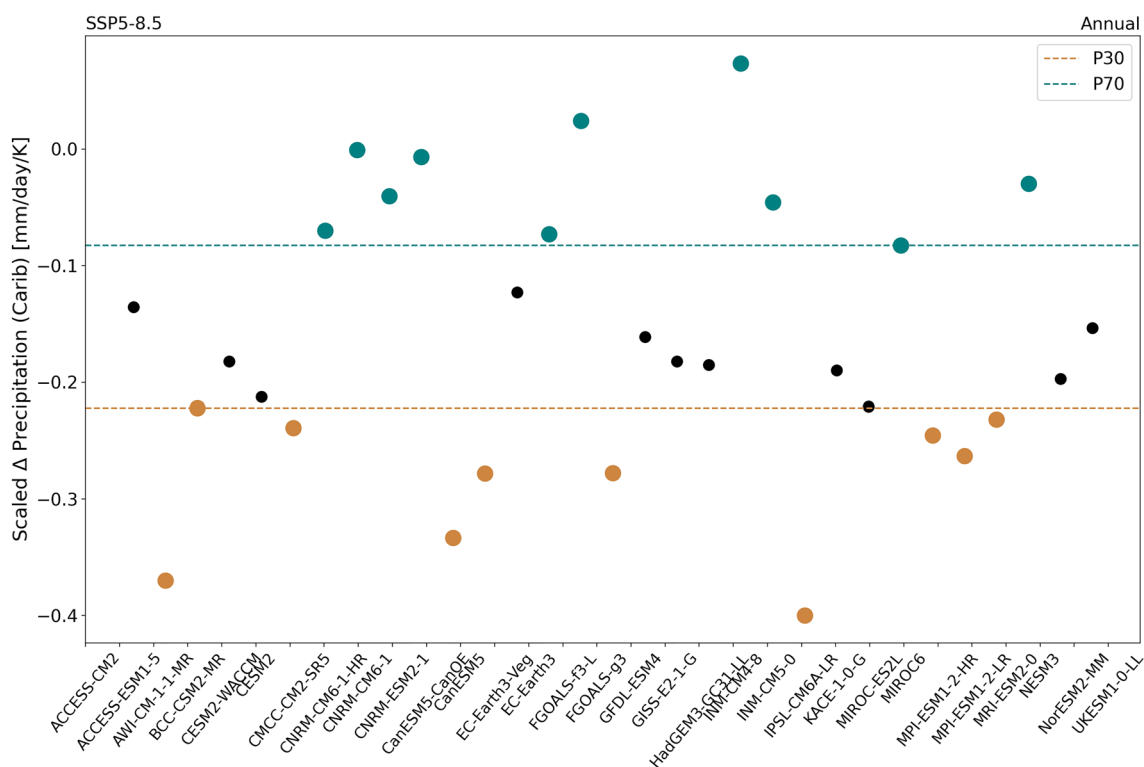


**Fig. 8** Scaled change in precipitation averaged over the Caribbean region (y-axis) for the 31 CMIP6 models (x-axis). The 30<sup>th</sup> and 70<sup>th</sup> percentiles of the 31 CMIP6 models' distribution are shown by the

brown and green dashed lines, respectively. The models defined as wet models are marked by green dots, while brown dots indicate the dry models

enhanced precipitation ranging from tropical South America in north-westerly direction is observed. Over the tropical Atlantic there is a clear dipole signal in both seasons indicating that dry models show a systematic poleward shift of the ITCZ compared to wet models.

Figure 10 shows the difference between dry and wet models for the scaled change in omega at 500 hPa (colors) and wind at 850 hPa (vectors) for the wet and dry seasons. Over the equatorial Pacific, a stronger upward movement (negative omega) is observed in dry models in both seasons. This indicates a stronger deep convection in dry models over the NPCZ. The location agrees with the enhanced precipitation seen in Fig. 9. Moreover, over the Caribbean, stronger downward motion is projected by dry models with a larger amplitude during the wet season. This stronger downward motion also enhances stronger trade winds over the Caribbean thereby enhancing the dryer conditions. Thus, the large difference between dry and wet models simulating the vertical motion in the Caribbean causes the large inter-model spread in precipitation projections during the wet season. Combined with the enhanced deep convection over the Pacific, we associate these changes with an eastward migration of the Walker circulation. For the dry season the difference in omega between dry and wet models over the Caribbean is,

however, minor, and unlikely to be the main cause between dry and wet models and points towards an important role for differences in moisture budget similar as for the model mean change. This will be further analyzed below. Over the tropical Atlantic a dipole in omega between dry and wet models is observed for the dry and wet seasons that matches with a shift in the ITCZ as noticed in Fig. 9.

Although there are notable differences Fig. 10 reveals a similar pattern as Fig. 5 indicating that similar changes in atmospheric circulation are responsible for the model mean drying as well as the inter-model spread.

#### 4.2.2 Moisture budget

Analyzing the moisture budget reveals that during the wet season the differences in moisture convergence between the dry and wet models are dominated by the mass convergence similar as for the model mean climate change (Fig. 17). For the dry season the difference in moisture convergence is less and dominated by the mass divergence although moisture advection contributes as well. Again, analogous results for the model mean climate change (Fig. 17) suggest similar mechanism explaining the multi-model mean and the inter-model spread.



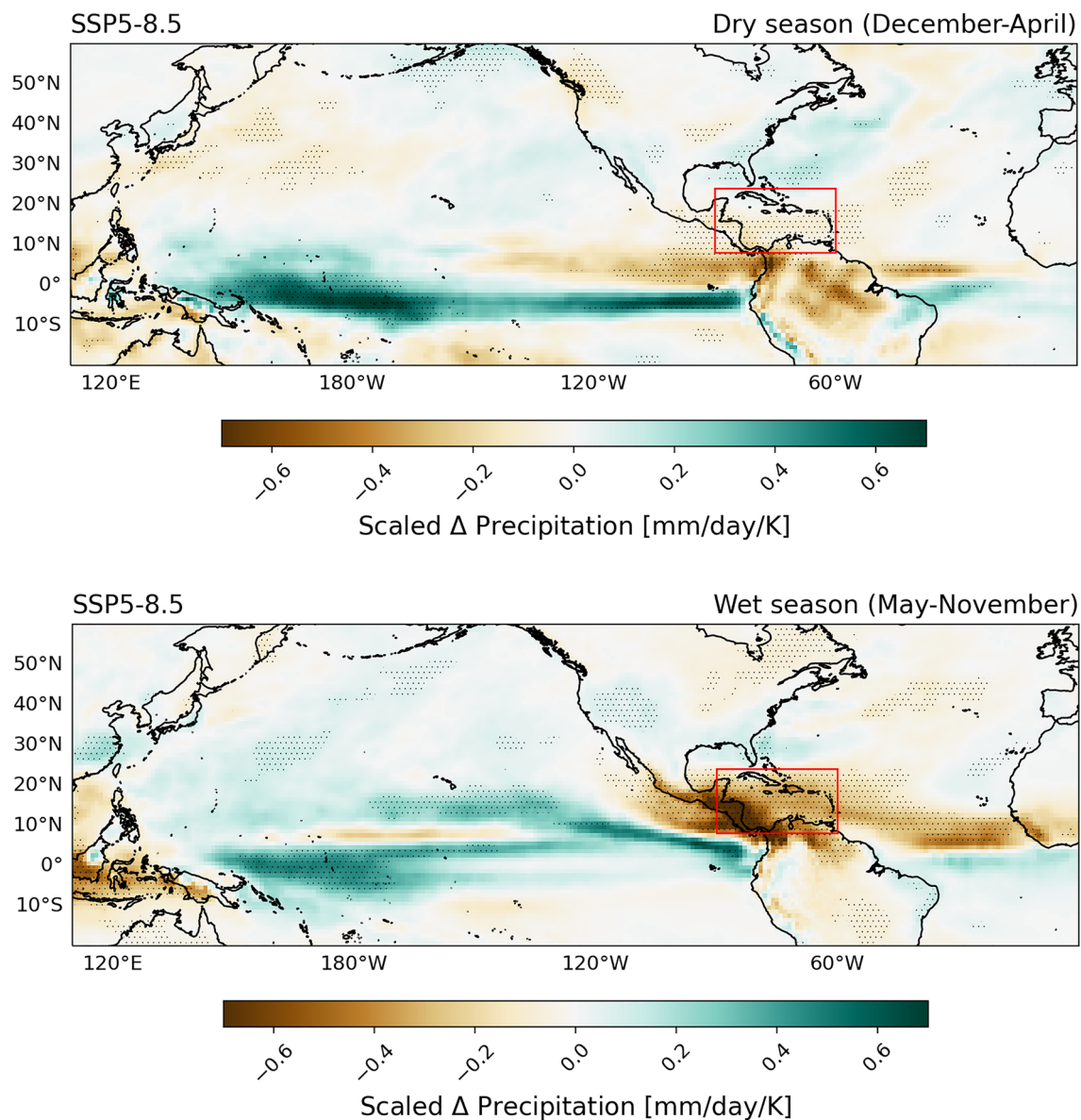


**Fig. 9** The difference between dry and wet models (multi-model mean dry models – multi-model mean wet models) for the scaled change in precipitation (*mm/day/K*). The dry and the wet seasons are

shown in the upper and lower panels, respectively. Hashing shows the regions where the difference is significant at the 95% confidence level. The red box shows the Caribbean region

### 4.2.3 Drivers of spread in Caribbean drying

The difference between dry and wet models for the scaled change in near surface temperature is shown in Fig. 19. Although also for the temperature pattern similarities between those for the model mean (Fig. 7) and inter-model spread (Fig. 19) can be observed, a much more detailed pattern is visible for the inter-model spread.

Different patterns can be identified, which can be linked to different atmospheric processes. Over the tropical Pacific, we see for both the dry and wet season a pattern similar to an El Niño or the positive phase of the Pacific Decadal

Oscillation (PDO). This suggests that the observed stronger eastward migration of the Walker circulation in the dry models, and accompanying subsidence over the Caribbean especially during the wet season is driven by this tropical Pacific warming. This is in agreement with the dominant role of El Niño explaining the interannual variability of precipitation over the Caribbean in present climate (Giannini et al. 2000; Martinez et al. 2020).

In the North Atlantic, more warming over the Gulf Stream and less warming south of Greenland, together with a dipole pattern over the tropical Atlantic are observed. The enhanced warming south of the equator and a weaker

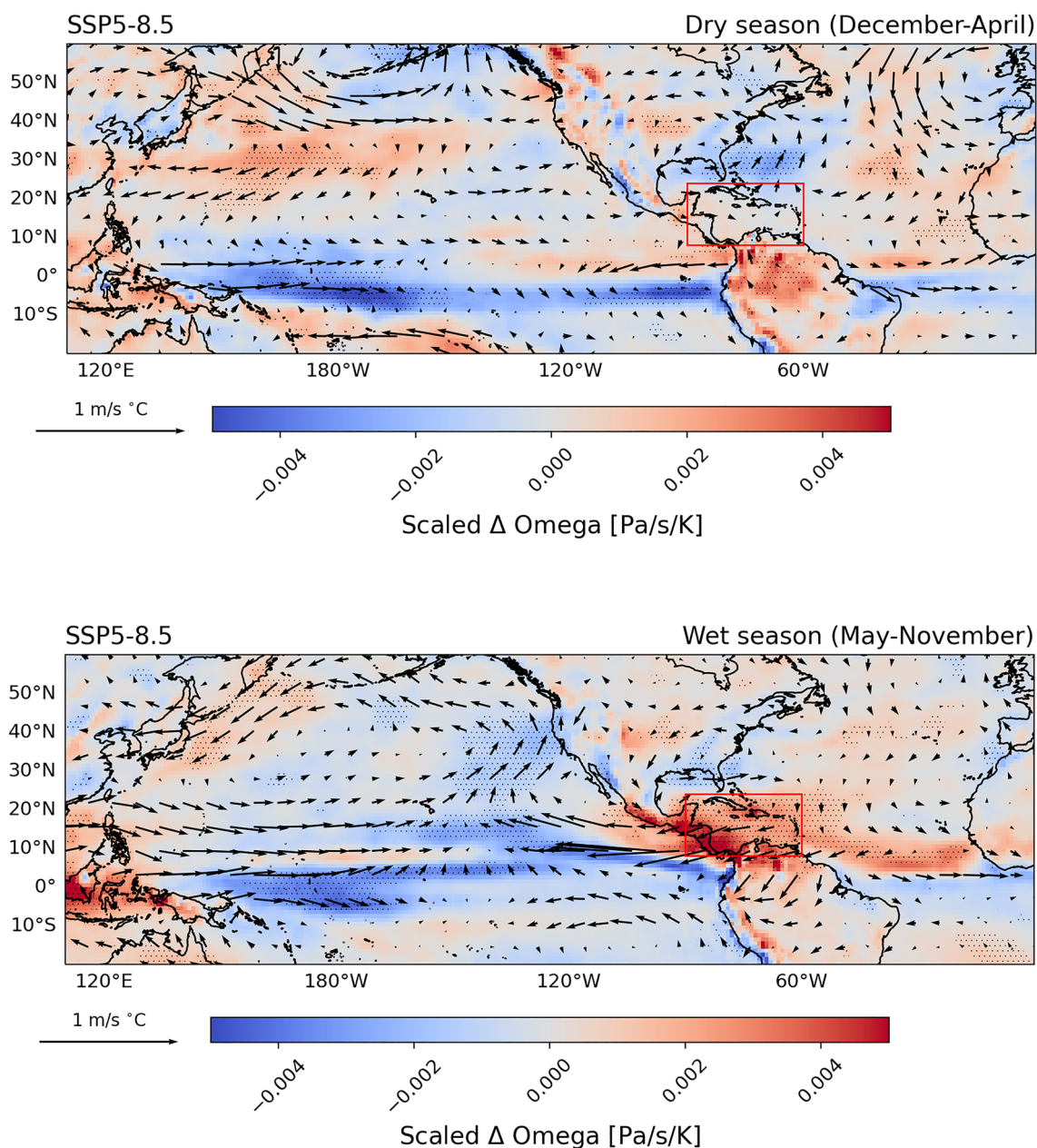


**Fig. 10** Same as Fig. 9 but for omega at 500 hPa (in colors, and in Pa/s/K) and wind at 850 hPa (in vectors and in m/s/K)

warming north of it (Fig. 19), induces a poleward shift of the ITCZ, as observed in Figs. 9 and 10, which is the dominant mechanism for drying during the dry season as revealed by the moisture budget analyses. Similar as for the model mean response, we speculate that larger (weaker) warming south (north) of the equator and southward (northward) shift of the ITCZ, is associated with the weak warming in the subpolar gyre and decline of the Atlantic meridional overturning circulation (AMOC), that affect the Atlantic meridional heat transport, between the dry and wet models. Further investigation of this mechanism is outside the scope of this paper.

A positive temperature difference is observed over the northern part of South America, which is more robust during the wet season. This, together with weaker warming over the Caribbean, indicates that dry models project a stronger temperature gradient between the Caribbean and the northern part of South America. Temperature gradients drive different flow patterns (Taylor et al. 2011). Hence, dry models project during the wet season a stronger divergent flow in the southern part of the Caribbean region (Fig. 10) induced by the enhanced Caribbean—South America temperature gradient.



Comparing the analyses of the inter-model spread with the multi-model mean change reveals that similar processes and drivers are responsible for the inter-model spread and model mean change. Although, also notable differences are observed with a much more detailed structure of the changes in the atmospheric circulation and the temperature warming for the inter-model spread (Fig. 11).

## 5 Emergent constraint analysis

From the results above, the importance of the Walker circulation for the multi-model mean and the inter-model spread of precipitation in the Caribbean is demonstrated, especially for the wet season. Moreover, it has been shown that this is linked to temperature changes in the tropical Pacific. As

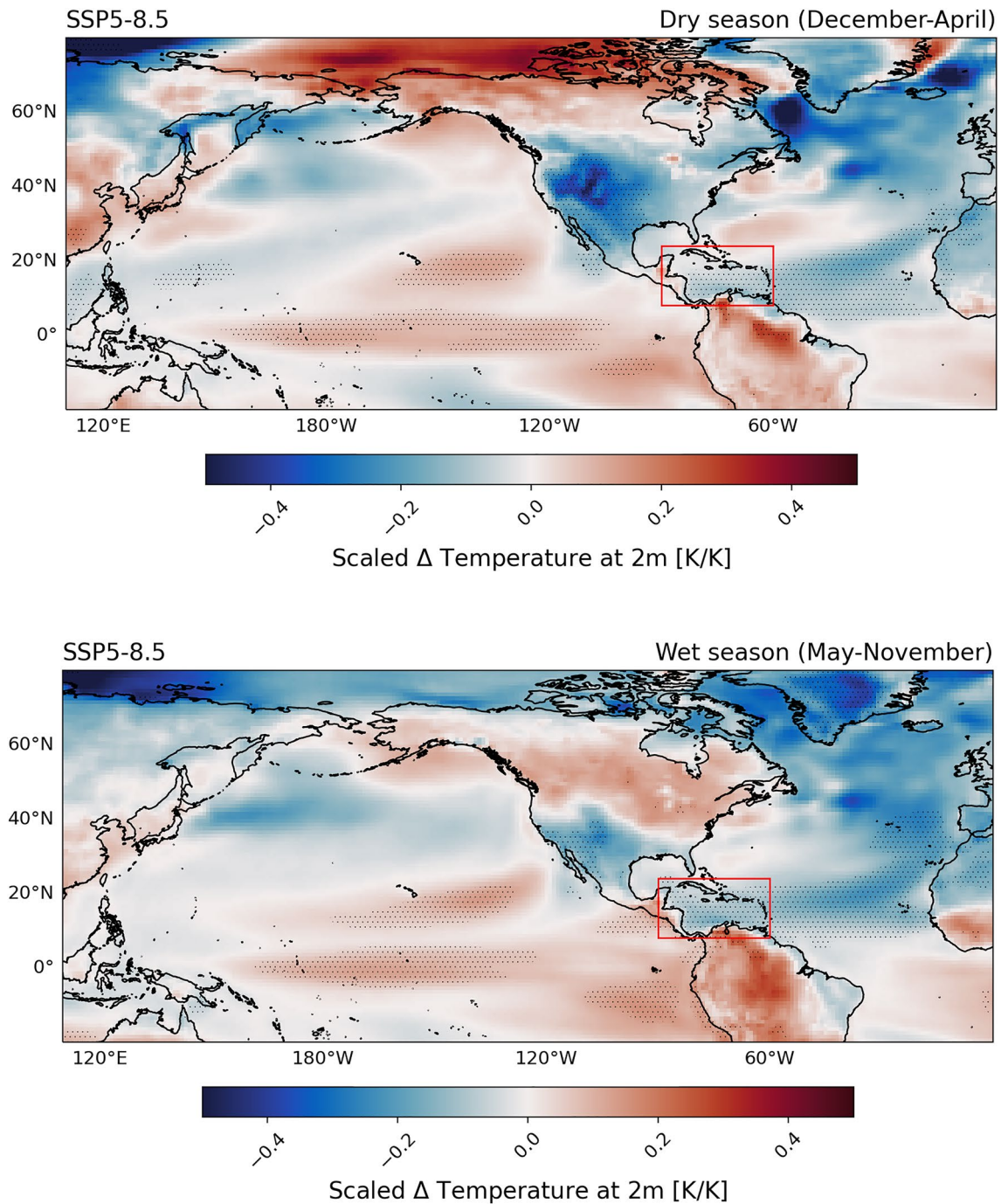
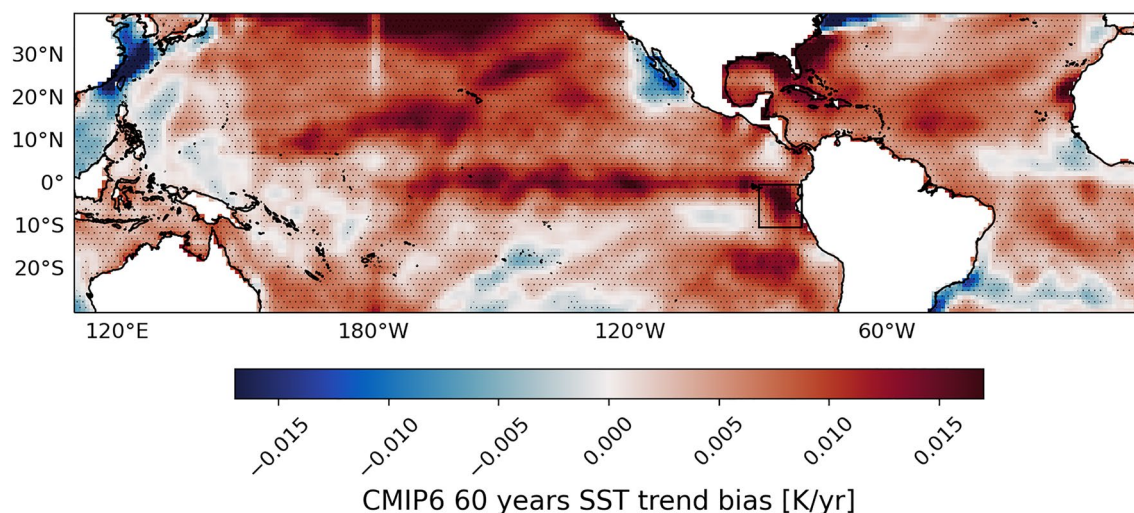


Fig. 11 Same as Fig. 9 but for temperature at 2 m (in K/K)

shown by Seager et al. (2019), CMIP5 models simulate a strong Niño 3.4 (region between 5°S to 5°N and 170°W to 120°W) warming trend over the past 60 years that is not seen in the observations (Fig. 1 in Seager et al. (2019)). Inspired by their work we calculated the difference between the observed and modeled 60 years SST trends. Figure 12 shows that the mismatch identified by Seager et al. (2019) is still present in CMIP6 models and is most prominent over the eastern tropical Pacific. On the other hand, over the western tropical Pacific the observations reveal a relative warming not simulated by the models. These results are in line with those of Wills et al. (2022) and are a long-standing problem (Bayr et al. 2014; Kociuba and Power 2015; Plesca et al. 2018). Moreover, this mismatch is not only present in climate models but has also been identified in different seasonal forecasting models. The amplitude of the difference in seasonal forecasting models is directly related to the lead time (Sharmila et al. 2023). Among the scientific community there is no clear consensus whether these discrepancies are produced by internal variability (Bayr et al. 2014; Plesca et al. 2018; Chung et al. 2019; Zhao and Allen 2019) or by a bias in the models (Kohyama et al. 2017; Seager et al. 2019, 2022; Wills et al. 2020, 2022; Suarez-Gutierrez et al. 2021). Understanding the drivers of this mismatch is not the scope of this research. However, the fact that none of the analyzed models (Fig. 18) are able to capture the observed trends suggests that the mismatch might be driven by a wrong representation of the real climate in the models. In addition, 60 years is a period of time long enough for the climate system to experience different long-period cycles, thus rejecting the possibility of natural variability causing these

discrepancies. Other studies (Seager et al. 2019, 2022; Wills et al. 2020, 2022) support this hypothesis. Consequently, the differences between the historical simulated and observed warming over the tropical Pacific makes the CMIP6 projections of future drying questionable.

We therefore investigate whether historical warming of the eastern tropical Pacific is related to future warming in that region in CMIP6 models. Figure 13a shows that there is indeed a strong relationship between present and future Niño 1 + 2 (region between 0°S to 10°S and 90°W to 80°W) warming in CMIP6 models. Because of the influence of eastern tropical Pacific warming on Caribbean rainfall we are able to apply an emergent constraint analysis for future Caribbean drying shown in Fig. 13b. The emergent constraint analysis reveals a negative correlation between present Niño 1 + 2 warming and future Caribbean drying. The Niño 1 + 2 is chosen because it is the region that shows the highest correlation with projected change of precipitation in the Caribbean and is also one of the areas where the SST trend bias is largest (Fig. 12). In Fig. 13, the wet season is shown because it is strongly influenced by Pacific SSTs. When comparing in Fig. 13b CMIP6 models (dots) with observations (vertical blue dashed line and shaded region), models show large trends with respect to observations, which is in line with the results found in Fig. 12. It is therefore impossible to constrain Caribbean precipitation projections with the equatorial Pacific SST trends since all the models are out of the range of the observed warming. In addition, the correlation between historical Niño 1 + 2 warming and future Caribbean drying is not very high ( $r = -0.55$ ) suggesting that other mechanisms (like the ones described along this



**Fig. 12** Multi-model mean of the 60 (1961–2020) years SST trend bias. Here the bias is defined as CMIP6 models—observations. Positive values indicate that CMIP6 models show a stronger warming trend compared to observations and vice-versa. The observed dataset

used is the HadISST. The Caribbean region is marked with a red box and the El Niño 1 + 2 is shown with a black box. Hashing shows the regions where the multi-model mean of the trend is significant at the 95% confidence level

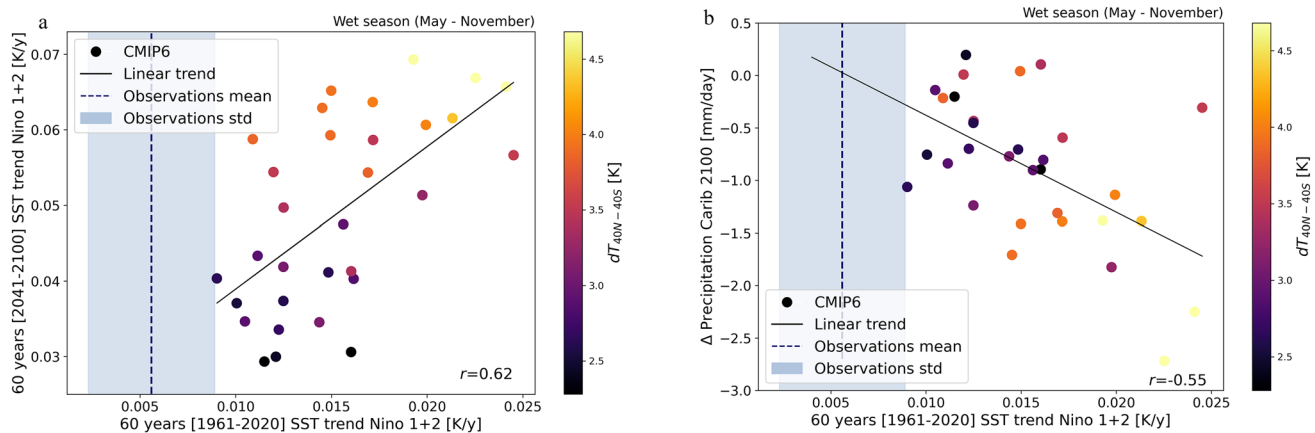


**Fig. 13** Emergent constraint analysis conformed by: scatterplot of simulated (a) historical (1961–2020) vs. future (2041–2100) Niño 1+2 60 years SST trends (in  $K/year$ ) and (b) historical (1961–2020) 60 years SST trends (in  $K/year$ ) vs. change in Caribbean precipitation (mm/day). Every point is one of the 31 CMIP6 models. The black line shows the linear trend between the x and y-axis for the CMIP6

manuscript) might be responsible for the remaining variability of precipitation in CMIP6 models. Therefore, we can not derive robust conclusions from this analysis. However, from Fig. 13b we can still state that future drying in the Caribbean will be likely weaker than the one projected by CMIP6 models. This result is supported by our physical understanding of the processes affecting precipitation in the Caribbean (described in Sect. 3). Moreover, similar emergent constraint analysis using different Niño regions (not shown) drive us to the same conclusion supporting this statement and increasing its confidence. Thus, we found a clear linkage between Caribbean drying and the equatorial Pacific SST trends bias. However, we did not find signs of a strong correlation between this bias and model resolution since model resolution is not related to Caribbean drying amplitude (Sect. 3.2.2, Table B.1).

To study the influence of climate sensitivity on the tropical Pacific warming and the Caribbean drying, we indicated in Fig. 13 with colors the projected  $40^{\circ}N - 40^{\circ}S$  warming for each model. Figure 13a, shows a linear relationship between the present and future Niño 1+2 warming with the projected global warming. This suggests climate sensitivity influences the simulated SST trends in the tropical Pacific. The association between projected global warming and drying in the Caribbean is not so clear in Fig. 13b. But a weak linear relationship can still be deduced suggesting that climate sensitivity might have some effect on the projected precipitation change in the Caribbean.

We found biases in the warming trends for CMIP6, but still an open question remains about the capability of the models to simulate the SST mean-state. The CMIP6 SST mean-state bias for the reference period is depicted in

models. The colors of the dots show the projected  $40^{\circ}N - 40^{\circ}S$  warming for every CMIP6 model.  $r$  refers to the Pearson Correlation Coefficient. The vertical dashed lines denote the mean, while the vertical blue shaded region shows the standard deviation of the historical observations of Niño 1+2 trend. The data sets used as observations are HadISST, ERA5 and ICOADS

Fig. 19a. During the historical period CMIP6 models simulate too high SSTs in the eastern equatorial Pacific which are largest on the Niño 1+2 region, while in the Caribbean, models simulate too low SSTs. The SST underestimation in the Caribbean has been previously addressed in CMIP5 models (Ryu and Hayhoe 2015). To understand the implications of the SSTs biases on the circulation we look at the omega bias (Fig. 19b). We observe that models simulate too strong downward flow over the Caribbean. These results suggest that not only Walker circulation trends are wrongly simulated by the models but also the mean-state. This leads us to conclude that CMIP6 simulations are dominated by a weak (or too eastward-located) Walker circulation, thus permanent enhanced El Niño conditions, which cause an overestimation of SSTs over the eastern equatorial Pacific and overestimation of the downward branch of the Walker cell over the Caribbean. These biases in the mean-state explain the region-wide underestimation of precipitation in the Caribbean (Fig. 3).

## 6 Discussion and conclusions

By analyzing an ensemble of 31 CMIP6 models, we found that the Caribbean precipitation is projected to decrease at the end of the twenty-first century. The amplitude of the drying differs among models leading to large inter-model uncertainty. The results shown in Sects. 3.1 and 3.2 indicate that the eastward migration of the Walker circulation is the process dominating both the drying trend and the inter-model spread during the wet season. The eastward migration of the Walker circulation drives subsidence over the



Caribbean, which produces moisture divergence and, therefore, drying. This circulation is similar as during El Niño events, whose effects on the Caribbean region have been previously studied (Giannini et al. 2000, 2001c; Martinez et al. 2020). During the dry season, the drying is dominated by mass divergence driven by the southward migration of the ITCZ and by the advection of dry air into the Caribbean. This applies for the model mean and the inter-model spread. We should note here that our approach has some limitations. In the first place, CMIP6 models' resolution is too coarse to properly resolve the islands and thus, some small-scale processes. Moreover, low-level atmospheric response cannot be captured by CMIP6 models. Thus, near surface moistening and orographic processes are absent. This may lead to an underestimation of precipitation, especially during boreal summer, due to the effect of orographic diurnal rainfall as shown by Jury and Bernard (2020). Investigating the impact of small-scale and low-level mechanisms on precipitation can only be achieved through dynamical downscaling, which is outside the scope of our work due to our interest on the general behavior of the models. Although, analyzing future CMIP6 climate with higher horizontal and vertical resolution methods seems an interesting path of research. In the second place, by averaging the Caribbean seasons in two (wet and dry) instead of four (WDS, ERS, MSD, LRS) we might underestimate some important processes as well. For example, Martinez et al. (2020) found NAO to be the dominant variability affecting precipitation during the ERS. Our approach could potentially obscure these kind of results. However, we decided to average over two seasons due to the large spread in CMIP6 models' precipitation simulations. These large inter-model differences suggest that CMIP6 are characterized by different climate regimes. Analyzing the individual models' climates is beyond the scope of this paper. Instead, our focus is on understanding the factors driving the multi-model mean and the variation between models. This argument underpins our choice of using two seasons rather than four. Nevertheless, a more detailed analysis with higher temporal resolution of CMIP6 is likely to yield valuable insights into the climate characteristics of individual models, which can enhance our understanding of Caribbean projections. This presents a promising line of research for further work. Additionally, caused by a heterogeneous precipitation distribution in the Caribbean (Martinez et al. 2019), examining the subregions independently would likely underscore the importance of other processes affecting precipitation. This can be as well considered as a new research opportunity.

In Sect. 3.3, we found that CMIP6 models are not able to properly simulate the tropical Pacific surface temperature trends for the historical period and associated changes in the Walker circulation in accordance with Wills et al. (2022). We also found a bias in the SST mean-state which suggests

that CMIP6 simulations are dominated by enhanced Niño conditions. These biases have no apparent correlation with the models' nominal resolutions. Over recent decades, a strengthening of the Walker circulation, related to a westward migration of the Walker circulation or La Niña-like dynamics, has been observed. In contrast, for the historical period, CMIP6 models simulate a warming of the eastern tropical Pacific, resembling an El Niño-like warming, together with a weakening and eastward migration of the Walker circulation. Although this issue has already been reported in previous versions of CMIP models (Bayr et al. 2014; Kociuba and Power 2015; Chung et al. 2019; Seager et al. 2019) and has also been confirmed for CMIP6 by Wills et al. (2022) a deeper investigation of this mismatch between observations and model simulations is still needed (Wang et al. 2021). Whether the mismatch in the modeled and observed Walker circulation trends is caused by natural variability or by a wrong simulation of the Pacific warming is still open to debate (Chung et al. 2019; Seager et al. 2019; Wills et al. 2022). We argue that natural variability is a less likely explanation since none of the models captures the observed SST trends and 60 year trends should be long enough to capture most of the variability of the climate system.

The strong influence of the tropical Pacific temperature on Caribbean precipitation and the tropical Pacific warming bias risk the reliability of Caribbean precipitation projections. Using an emergent constraint analysis where we correlate historical Niño 1+2 SST trends with future Caribbean precipitation we try to constraint projections. However, a confident quantitative constraint of the Caribbean precipitation results impossible from this analysis due to a twofold reason. First, although the physical understanding of the link between tropical Pacific SSTs and Caribbean precipitation is clear and has already been reported in the bibliography (Giannini et al. 2000, 2001a, b, c; Martinez et al. 2019), the correlation between these two is not robust enough in our results. Second, the discrepancies between modeled and observed SST trends are so large that none of the models fall in the observed range. Therefore, more research is needed in order to be able to confidently constraint precipitation projections in the Caribbean. Nevertheless, we can still state that at the end of the century the drying in the Caribbean will probably have a weaker amplitude than in CMIP6 projections. The projected Caribbean drying might be weakly influenced by climate sensitivity. The conclusions are in line with our understanding of the drivers of Caribbean precipitation.

Another field of research that may be impacted by the mismatch between observed and simulated changes in the Walker circulation, is the field of tropical cyclone (TC) research. TC formation is directly influenced by vertical windshear, where high values of vertical windshear decrease

TC formation chances. This means that typically, during El Niño years, TC formation may be lower (Vecchi and Soden 2007). As such, following our previously obtained results, the over-representation of El Niño circulation in CMIP6 models may result in an underestimation of TC frequencies (and hence also TC probabilities of occurrence at the local scale, as was for instance found in Bloemendaal et al. (2022)) in the Caribbean region under future warming.

**Supplementary Information** The online version contains supplementary material available at <https://doi.org/10.1007/s00382-023-07072-3>.

**Funding** This project has received funding from European Union's Horizon 2020 Research and Innovation Programme under Grant Agreement No 101073954 (<https://www.paratus-project.eu>).

**Data availability** The MSWEP can be downloaded from <https://www.gloh2o.org/mswep/> under request. The GPCP monthly mean precipitation observations data is available at <https://psl.noaa.gov/data/gridded/data.gpcp.html>. The ERA5 reanalysis data was downloaded from <https://cds.climate.copernicus.eu/cdsapp#!/home>. The HadISST and ICOADS SST datasets are available at <https://www.metoffice.gov.uk/hadobs/hadisst/data/download.html> and <https://psl.noaa.gov/data/gridded/data.coads.1.deg.html>, respectively. The CMIP6 models' output is available at <https://esgf-node.llnl.gov/projects/cmip6/>.

## Declarations

**Conflict of interest** The authors declare that they have no conflicts of interest.

**Open Access** This article is licensed under a Creative Commons Attribution 4.0 International License, which permits use, sharing, adaptation, distribution and reproduction in any medium or format, as long as you give appropriate credit to the original author(s) and the source, provide a link to the Creative Commons licence, and indicate if changes were made. The images or other third party material in this article are included in the article's Creative Commons licence, unless indicated otherwise in a credit line to the material. If material is not included in the article's Creative Commons licence and your intended use is not permitted by statutory regulation or exceeds the permitted use, you will need to obtain permission directly from the copyright holder. To view a copy of this licence, visit <http://creativecommons.org/licenses/by/4.0/>.

## References

- the Earth, Part B: Hydrology, Oceans and Atmosphere 26.2, pp. 143–147. Giannini, Alessandra, Mark A Cane, and Yochanan Kushnir (2001b). "Interdecadal changes in the ENSO teleconnection to the Caribbean region and the North Atlantic Oscillation". In: *Journal of Climate* 14.13, pp. 2867–2879.
- Adam O, Schneider T, Briant F (2020) Regional and seasonal variations of the double-ITCZ bias in CMIP5 models. *Clim Dyn* 51:101–117
- Adams DK, Andrew CC (1997) The north American monsoon. *Bull Am Meteorol Soc* 78(10):2197–2214
- Alexander MA et al (2002) The atmospheric bridge: The influence of ENSO teleconnections on air–sea interaction over the global oceans. *J Clim* 15(16):2205–2231

- Allen TL, Brian EM (2017) The late spring Caribbean rain-belt: climatology and dynamics. *Int J Climatol* 37(15):4981–4993
- Almazroui M et al (2021) Projected changes in temperature and precipitation over the United States, Central America, and the Caribbean in CMIP6 GCMs. *Earth Syst Environ* 5:1–24
- Angeline P (2016) The climate data guide: GPCP (Monthly): Global precipitation climatology project. In: National Center for Atmospheric Research Staff (Eds), Last modified 2.
- Anthony CA, Michael AT (2002) Investigating the link between early season Caribbean rainfall and the El Niño+ 1 year. *Int J Climatol: A Jf the Royal Meteorological Society* 22.1, pp. 87–106.
- Bayr T et al (2014) The eastward shift of the Walker Circulation in response to global warming and its relationship to ENSO variability. *Clim Dyn* 43:2747–2763
- Beck, Hylke E et al. (2019). "MSWEP V2 global 3-hourly 0.1 precipitation: methodology and quantitative assessment". In: *Bulletin of the American Meteorological Society* 100.3, pp. 473–500.
- Bellomo, Katinka et al. (2021). "Future climate change shaped by inter-model differences in Atlantic meridional overturning circulation response". In: *Nature Communications* 12.1, p. 3659.
- Bloemendaal, Nadia and EE Koks (2022). "Current and Future Tropical Cyclone Wind Risk in the Small Island Developing States". In: *Hurricane Risk in a Changing Climate*. Springer, pp. 121–142.
- Bloemendaal, Nadia et al. (2022). "A globally consistent local-scale assessment of future tropical cyclone risk". In: *Science advances* 8.17, eabm8438.
- Brogli, Roman et al. (2021). "Future summer warming pattern under climate change is affected by lapse-rate changes". In: *Weather and Climate Dynamics* 2.4, pp. 1093–1110.
- Caesar, Levke et al. (2018). "Observed fingerprint of a weakening Atlantic Ocean overturning circulation". In: *Nature* 556.7700, pp. 191–196.
- Centella-Artola, Abel et al. (2020). "Evaluation of sixteen gridded precipitation datasets over the Caribbean region using gauge observations". In: *Atmosphere* 11.12, p. 1334.
- Chang, Y-L and L-Y Oey (2013). "Coupled response of the trade wind, SST gradient, and SST in the Caribbean Sea, and the potential impact on Loop Current's interannual variability". In: *Journal of Physical Oceanography* 43.7, pp. 1325–1344.
- Chung, Eui-Seok et al. (2019). "Reconciling opposing Walker circulation trends in observations and model projections". In: *Nature Climate Change* 9.5, pp. 405–412. Climate Studies Group Mona (Eds.) (2020). *The State of the Caribbean Climate*. url: <https://www.caribank.org/publications-and-resources/resource-library/publications/state-caribbean-climate> (visited on 10/08/2022).
- Cook, Kerry H and Edward K Vizy (2010). "Hydrodynamics of the Caribbean low-level jet and its relationship to precipitation". In: *Journal of Climate* 23.6, pp. 1477–1494.
- Cook, Benjamin I et al. (2020). "Twenty-first century drought projections in the CMIP6 forcing scenarios". In: *Earth's Future* 8.6, e2019EF001461.
- Drijfhout, Sybren, Geert Jan Van Oldenborgh, and Andrea Cimatoribus (2012). "Is a decline of AMOC causing the warming hole above the North Atlantic in observed and modeled warming patterns?" In: *Journal of Climate* 25.24, pp. 8373–8379.
- Eyring, Veronika et al. (2016). "Overview of the Coupled Model Intercomparison Project Phase 6 (CMIP6) experimental design and organization". In: *Geoscientific Model Development* 9.5, pp. 1937–1958.
- Freeman, Eric et al. (2017). "ICOADS Release 3.0: a major update to the historical marine climate record". In: *International Journal of Climatology* 37.5, pp. 2211–2232.
- Giannini, Alessandra, Yochanan Kushnir, and Mark A Cane (2000). "Interannual variability of Caribbean rainfall, ENSO, and the Atlantic Ocean". In: *Journal of Climate* 13.2, pp. 297–311.



- Giannini, A, Y Kushnir, and MA Cane (2001a). “Seasonality in the impact of ENSO and the North Atlantic high on Caribbean rainfall”. In: *Physics and Chemistry of*
- Giannini, Alessandra et al. (2001c). “The ENSO teleconnection to the tropical Atlantic Ocean: Contributions of the remote and local SSTs to rainfall variability in the tropical Americas”. In: *Journal of Climate* 14.24, pp. 4530–4544.
- Goldenberg, Stanley B and Lloyd J Shapiro (1996). “Physical mechanisms for the association of El Niño and West African rainfall with Atlantic major hurricane activity”. In: *Journal of Climate* 9.6, pp. 1169–1187.
- Gray, William M (1984). “Atlantic seasonal hurricane frequency. Part I: El Niño and 30 mb quasi-biennial oscillation influences”. In: *Monthly weather review* 112.9, pp. 1649–1668.
- Gu, Guojun, Robert F Adler, and Adam H Sobel (2005). “The eastern Pacific ITCZ during the boreal spring”. In: *Journal of the atmospheric sciences* 62.4, pp. 1157–1174.
- Herrera, Dimitris A et al. (2020). “Projected hydroclimate changes on Hispaniola Island through the 21st century in CMIP6 Models”. In: *Atmosphere* 12.1, p. 6.
- Holland, Marika M and Cecilia M Bitz (2003). “Polar amplification of climate change in coupled models”. In: *Climate dynamics* 21.3–4, pp. 221–232.
- Joshi MM et al (2008) Mechanisms for the land/sea warming contrast exhibited by simulations of climate change. *Clim Dyn* 30:455–465
- Jury MR, Bernard D (2020) Climate trends in the east Antilles islands. *Int J Climatol* 40(1):36–51
- Karmalkar, Ambarish V et al. (2013). “A review of observed and projected changes in climate for the islands in the Caribbean”. In: *Atm´osfera* 26.2, pp. 283–309
- Klotzbach, Philip J (2011a). “El Niño–Southern Oscillation’s impact on Atlantic basin hurricanes and US landfalls”. In: *Journal of Climate* 24.4, pp. 1252–1263.
- Klotzbach, Philip J (2011b). “The influence of El Niño–Southern Oscillation and the Atlantic multidecadal oscillation on Caribbean tropical cyclone activity”. In: *Journal of Climate* 24.3, pp. 721–731.
- Kociuba, Greg and Scott B Power (2015). “Inability of CMIP5 models to simulate recent strengthening of the Walker circulation: Implications for projections”. In: *Journal of Climate* 28.1, pp. 20–35.
- Kohyama, Tsubasa, Dennis L Hartmann, and David S Battisti (2017). “La Niña-like mean-state response to global warming and potential oceanic roles”. In: *Journal of Climate* 30.11, pp. 4207–4225.
- Lewsey, Clement, Gonzalo Cid, and Edward Kruse (2004). “Assessing climate change impacts on coastal infrastructure in the Eastern Caribbean”. In: *Marine Policy* 28.5, pp. 393–409.
- Martin, Elinor R and Courtney Schumacher (2011). “Modulation of Caribbean precipitation by the Madden–Julian oscillation”. In: *Journal of Climate* 24.3, pp. 813–824.
- Martinez C et al (2019) Seasonal climatology and dynamical mechanisms of rainfall in the Caribbean. *Clim Dyn* 53:825–846
- Martinez C et al (2020) Interannual variability of the early and late-rainy seasons in the Caribbean. *Clim Dyn* 55:1563–1583
- Masson-Delmotte, VP et al. (2021). “Ipcc, 2021: Summary for policymakers. in: *Climate change 2021: The physical science basis. contribution of working group i to the sixth assessment report of the intergovernmental panel on climate change*”. In: *Mendez, Mat´ias and V´ictor Maga˜na* (2010). “Regional aspects of prolonged meteorological droughts over Mexico and Central America”. In: *Journal of Climate* 23.5, pp. 1175–1188.
- Van Meerbeek, C. (2020). *Climate Trends and Projections for the OECs Region*. url: <https://www.oecs.org/en/our-work/knowledge/library/climate-change/climate-trends-and-projections-for-the-oecs-region> (visited on 10/08/2022).
- Philander, SGH et al. (1996). “Why the ITCZ is mostly north of the equator”. In: *Journal of climate* 9.12, pp. 2958–2972.
- Pithan, Felix and Thorsten Mauritsen (2014). “Arctic amplification dominated by temperature feedbacks in contemporary climate models”. In: *Nature geoscience* 7.3, pp. 181–184.
- Plesca, Elina, Verena Gru’tzun, and Stefan A Buehler (2018). “How robust is the weakening of the Pacific Walker circulation in CMIP5 idealized transient climate simulations?” In: *Journal of Climate* 31.1, pp. 81–97.
- Rahmstorf, Stefan et al. (2015). “Exceptional twentieth-century slowdown in Atlantic Ocean overturning circulation”. In: *Nature climate change* 5.5, pp. 475–480.
- Rayner, NAA et al. (2003). “Global analyses of sea surface temperature, sea ice, and night marine air temperature since the late nineteenth century”. In: *Journal of Geophysical Research: Atmospheres* 108.D14.
- Rodríguez-Vera, Geidy et al. (2019). “Coupled interannual variability of wind and sea surface temperature in the Caribbean Sea and the Gulf of Mexico”. In: *Journal of Climate* 32.14, pp. 4263–4280.
- Ryu J-H, Hayhoe K (2015) Regional and large-scale influences on seasonal to interdecadal variability in Caribbean surface air temperature in CMIP5 simulations. *Clim Dyn* 45:455–475
- Santer, Benjamin D et al. (1990). “Developing climate scenarios from equilibrium GCM results”. In:
- Seager, Richard, Naomi Henderson, and Mark Cane (2022). “Persistent discrepancies between observed and modeled trends in the tropical Pacific Ocean”. In: *Journal of Climate* 35.14, pp. 4571–4584.
- Seager, Richard et al. (2019). “Strengthening tropical Pacific zonal sea surface temperature gradient consistent with rising greenhouse gases”. In: *Nature Climate Change* 9.7, pp. 517–522.
- Sharmila, S et al. (2023). “Contrasting El Niño–La Niña Predictability and Prediction Skill in 2-Year Reforecasts of the Twentieth Century”. In: *Journal of Climate* 36.5, pp. 1269–1285.
- Si, Wei et al. (2021). “Double Intertropical Convergence Zones in Coupled Ocean–Atmosphere Models: Progress in CMIP6”. In: *Geophysical Research Letters* 48.23, pp. 1–8. issn: 0094–8276. doi: <https://doi.org/10.1029/2021gl094779>.
- Suarez-Gutierrez, Laura, Sebastian Milinski, and Nicola Maher (2021). “Exploiting large ensembles for a better yet simpler climate model evaluation”. In: *Climate Dynamics* 57.9–10, pp. 2557–2580.
- Tartaglione, Carissa A, Shawn R Smith, and James J O’Brien (2003). “ENSO impact on hurricane landfall probabilities for the Caribbean”. In: *Journal of Climate* 16.17, pp. 2925–2931.
- Taylor, Michael A, David B Enfield, and A Anthony Chen (2002). “Influence of the tropical Atlantic versus the tropical Pacific on Caribbean rainfall”. In: *Journal of Geophysical Research: Oceans* 107.C9, pp. 10–1.
- Taylor, Michael A et al. (2011). “Tropical gradient influences on Caribbean rainfall”. In: *Journal of Geophysical Research: Atmospheres* 116.D21.
- Taylor, Michael A et al. (2012). “Climate change and the Caribbean: Review and response”. In: *Caribbean studies*, pp. 169–200.
- Tian, Baijun and Xinyu Dong (2020). “The double-ITCZ bias in CMIP3, CMIP5, and CMIP6 models based on annual mean precipitation”. In: *Geophysical Research Letters* 47.8, e2020GL087232.
- Vecchi, Gabriel A and Brian J Soden (2007). “Global warming and the weakening of the tropical circulation”. In: *Journal of Climate* 20.17, pp. 4316–4340.
- Visbeck, Martin H et al. (2001). “The North Atlantic Oscillation: past, present, and future”. In: *Proceedings of the National Academy of Sciences* 98.23, pp. 12876–12877.
- Waliser, Duane E and Catherine Gautier (1993). “A satellite-derived climatology of the ITCZ”. In: *Journal of climate* 6.11, pp. 2162–2174.
- Wang C (2007) Variability of the Caribbean low-level jet and its relations to climate. *Clim Dyn* 29:411–422

- Wang, Chunzai and Sang-ki Lee (2007). "Atlantic warm pool, Caribbean low-level jet, and their potential impact on Atlantic hurricanes". In: *Geophysical research letters* 34.2.
- Wang, Chunzai, Sang-Ki Lee, and David B Enfield (2008). "Climate response to anomalously large and small Atlantic warm pools during the summer". In: *Journal of Climate* 21.11, pp. 2437–2450.
- Wang, Xin-Yue et al. (2021). "Underestimated responses of Walker circulation to ENSO-related SST anomaly in atmospheric and coupled models". In: *Geoscience Letters* 8.1, pp. 1–13.
- Wills, Robert CJ et al. (2020). "Pattern recognition methods to separate forced responses from internal variability in climate model ensembles and observations". In: *Journal of Climate* 33.20, pp. 8693–8719.
- Wills, Robert CJ et al. (2022). "Systematic Climate Model Biases in the Large-Scale Patterns of Recent Sea-Surface Temperature and Sea-Level Pressure Change". In: *Geophysical Research Letters* 49.17, e2022GL100011.
- Zhang, Xiaoxiao, Hailong Liu, and Minghua Zhang (2015). "Double ITCZ in Coupled Ocean-Atmosphere Models: From CMIP3 to CMIP5". In: *Geophysical Research Letters* 42.20, pp. 8651–8659. issn: 19448007. doi: <https://doi.org/10.1002/2015GL065973>.
- Zhang, Chidong (2001). "Double ITCZs". In: *Journal of Geophysical Research: Atmospheres* 106.D11, pp. 11785–11792.
- Zhao, Xueying and Robert J Allen (2019). "Strengthening of the Walker Circulation in recent decades and the role of natural sea surface temperature variability". In: *Environmental Research Communications* 1.2, p. 021003.

**Publisher's Note** Springer Nature remains neutral with regard to jurisdictional claims in published maps and institutional affiliations.